9th International Conference on Fracture Mechanics of Concrete and Concrete Structures
FraMCoS-9
V. Saouma, J. Bolander, and E. Landis (Eds)

DOI 10.21012/FC9.074

EFFECTS OF MICROCRACKS IN THE INTERFACIAL ZONE ON THE MACRO BEHAVIOR OF CONCRETE

KEERTHY M. SIMON* **AND J. M. CHANDRA KISHEN†**

*Graduate student, Indian Institute of Science
Bangalore, India
e-mail: keerthym@civil.iisc.ernet.in

†Professor, Indian Institute of Science
Bangalore, India
e-mail: chandrak@civil.iisc.ernet.in

Key words: Interfacial transition zone, Microcrack, Post-peak response, Concrete

Abstract. The existence of microcracks influences the macroscopic behavior of quasibrittle materials like concrete. This study aims at predicting the post-peak response of concrete by considering the effect of microcracks, by quantifying the critical microcrack length. The critical length of a microcrack is estimated by considering a small element near the macro crack tip and thereby defining the critical crack opening displacement of the micro crack, that exists in the interface region between the aggregate and cement paste. The ratio of critical microcrack to the specimen depth is found to be constant for a particular mix of concrete and can be used as a material property. The predicted post-peak response of plain concrete beams is validated using experimental data available in the literature. Through a sensitivity analysis, it is observed that the elastic modulus of concrete and the fracture toughness of the interface has a substantial influence on the critical microcrack length.

1 Introduction

Concrete, one of the most widely used construction materials, is treated as homogeneous from a design perspective. However, on a close meso level examination it is observed that the internal structure is heterogeneous, consisting of coarse aggregates embedded in cement matrix. Upon magnification of the matrix material, the coexistence of fine aggregate and cement paste can be seen as shown in Figure 1. Further, there exists a region, which is known as the interfacial transition zone (ITZ) that occurs between the cement paste and aggregates. The cement paste and aggregates are bonded at the interface whose strength depends on its microstructural characteristics.

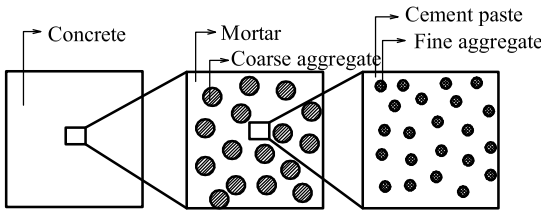

Figure 1: Structure of concrete.

In fresh concrete, the cement particles cannot pack together efficiently when they are in the close vicinity of a larger object such as aggregate. During mixing of concrete, the shearing stress exerted on the cement paste by the aggregates tends to separate water from cement particles and results in a small region around the aggregate particles with fewer cement particles termed as the ITZ [1]. The existence

of a thin film of hydrated constituents was observed by Farran [1] in 1953 around the aggregate upon hardening of concrete. The composition of this zone was found to be different from that of cement paste as the density of cement particles were lesser than that of its surroundings. Although several techniques such as X-ray diffraction, X-ray photoelectron spectroscopy, secondary ion mass spectroscopy, mercury intrusion porosimetry, optical microscope and electron microscope have been employed to study the ITZ, the complete characterization of the distinctive features of this zone has still not been achieved. The interface acts as a bridge between aggregate and the cement paste which neither possesses the properties of aggregate nor the cement paste.

Upon loading, microcracking initiates in the ITZ when the local major principal stress exceeds the initial tensile strength of the interface [2]. Ansari [3] reported that the macrocrack will occur only when the microcrack reaches a critical length. This critical microcrack length propagates and coalesces with existing macrocrack thereby resulting in the failure of the bond. The stiffness of the interface decreases although the individual components on either side of the interface possess high stiffness. This is due to the presence of voids and microcracks in this region which do not allow the transfer of stress.

The packing and density of the cement particle around the aggregates defines the strength of the interfacial zone. The strength of an interface decides whether a crack should grow around an aggregate particle, or through the aggregate. Also, the fracture energy of the interface is found to be less than that of the cement paste and aggregate. The micro structural character of the interfacial zone governs the mode I crack propagation in concrete [4]. Thus, the material behavior of concrete is influenced by the geometry, the spatial distribution and the material property of the individual material constituents and their mutual interaction. Hence, the failure of concrete structure can be viewed as a multiscale phenomenon, where in, the information of the material properties at a micro level can be used to determine the system behavior at the macro level.

In this paper, the effects of ITZ and the microcracks on the overall behavior of concrete are studied by estimating the critical length of the microcracks present in the ITZ using the principles of linear elastic fracture mechanics. A procedure to determine the material properties at the ITZ including the elastic modulus and the fracture toughness by knowing the mix proportions of the ingredients in concrete is explained. Using the information of the critical microcrack length, an analytical model is proposed through a relationship between the applied stress and the crack opening displacement to obtain the macro behavior of the material. The proposed analytical model is validated using experimental data and the results of various investigators that are published in the literature for normal strength concrete. Furthermore, since various parameters are involved in the determination of the critical microcrack length, which is randomly distributed, sensitivity analysis is done to study the most sensitive parameter which affects the microcrack size.

2 Critical microcrack length

The initiation and propagation of microcrack at the interface between the cement paste and the aggregates is attributed to the toughness of the interface. In this study, the critical microcrack length is a parameter which is used to characterize the interface. As the critical microcrack length increases, the toughness of the interface increases and there by contributing to the overall strength of concrete. The existence of microcrack and restraining stress at the macrocrack tip is a well known fact. Upon loading, the microcrack will initiate at the interface and later coalesce with the existing macrocrack resulting in the crack increment. In this study, the critical length of the microcrack is determined by analyzing a small element near the macrocrack tip and along the interface between the cement paste and aggregate, as depicted in Figure 2.

The following assumptions are made in the derivation of the critical microcrack length: (1)

The microcrack grows in a direction perpendicular to the maximum principal stress. (2) The initial microcrack length is assumed to be much smaller than the size of the element considered. (3) The microcrack tip is sharp for linear elastic fracture mechanics to be applied.

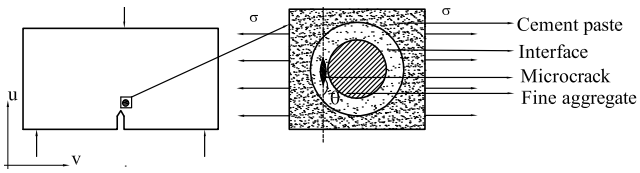

Figure 2: Representation of microcrack at interface.

The stresses and displacement along the crack tip for this two-dimensional crack problem is determined through an inverse method by making use of an Airy stress function (ϕ), which satisfies the biharmonic equation ($\nabla^2\nabla^2\phi = 0$). The stresses and strains in the polar coordinate system are further determined. Using these strains, the displacements in the polar coordinate system are obtained as

$$V_r = \frac{1}{2\mu_{micro}} \sum_{n=0}^{\infty} r^{\lambda_n} \Big[-(\lambda_n + 1) B_n cos(\lambda_n + 1)\theta + D_n cos(\lambda_n - 1)\theta \Big\{ \frac{4}{1+\nu_{micro}} - (\lambda_n + 1) \Big\} \Big]$$

$$V_\theta = \frac{1}{2\mu_{micro}} \sum_{n=0}^{\infty} r^{\lambda_n} \Big[-(\lambda_n + 1) B_n sin(\lambda_n + 1)\theta + D_n sin(\lambda_n - 1)\theta \Big\{ \frac{4}{1+\nu_{micro}} + (\lambda_n - 1) \Big\} \Big] \quad (1)$$

In the above equations, μ_{micro} and ν_{micro} are the shear modulus and the Poisson's ratio of the interface respectively, where the microcrack is likely to occur. The microcrack present in the interface is assumed to be sharp in order to initiate the crack propagation. The crack surface of the microcrack is considered as stress free and the corresponding boundary conditions along the upper surface denoted by (+) and lower surface (-) are given by

$$\sigma_{\theta\theta} = \sigma_{r\theta} = 0, \theta = \pm\pi \quad (2)$$

Assuming the microcrack to be very sharp, the microcrack angle attains a value of π and the characteristic equation reduces to $sin(2\lambda_n\pi) = 0$. The roots of this characteristic equation gives the eigenvalues ($\lambda_n = \frac{n}{2}; n = 0 \pm 1 \pm 2, ..$). The crack tip singularity is observed when the eigenvalue becomes 0.5. The displacement field near the microcrack tip reduces to the following form

$$V_r = \frac{r^{1/2}}{2\mu_{micro}} \Big[-\Big(\frac{1}{2}+1\Big) B_1 cos\Big(\frac{1}{2}+1\Big)\theta - \Big(\frac{1}{2}+1\Big) D_1 cos\Big(\frac{1}{2}-1\Big)\theta + \Big(\frac{4}{1+\nu_{micro}}\Big) D_1 cos\Big(\frac{1}{2}-1\Big)\theta \Big] \quad (3)$$

$$V_\theta = \frac{r^{1/2}}{2\mu_{micro}} \Big[\Big(\frac{1}{2}+1\Big) B_1 sin\Big(\frac{1}{2}+1\Big)\theta + \Big(\frac{1}{2}-1\Big) D_1 sin\Big(\frac{1}{2}-1\Big)\theta + \Big(\frac{4}{1+\nu_{micro}}\Big) D_1 sin\Big(\frac{1}{2}-1\Big)\theta \Big] \quad (4)$$

A relationship between B_1 and D_1 is obtained by substituting the eigenvalue into the boundary condition ($B_1 = D_1/3$). This reduces the displacement field in terms of one unknown parameter D_1. Further, by defining $D_1 = K_1/\sqrt{2\pi}$, the displacement field becomes a function of stress intensity factor (K).

The crack opening displacement corresponding to the microcrack is determined by transforming the displacement component perpendicular to the loading direction (V) into rectangular coordinates by making use of the following transformation

$$V = V_r sin(\theta) + V_\theta cos(\theta) \quad (5)$$

By substituting $\theta = +\beta^*$ and $\theta = -\beta^*$ the displacement field along the upper (V^+) and the lower (V^-) surface of the crack is obtained. The corresponding displacement fields are given by

$$V^+ = V_r sin(\theta) + V_\theta cos(\theta)\Big|_{\theta=+\beta^*} \quad (6)$$

$$V^- = V_r sin(\theta) + V_\theta cos(\theta)\Big|_{\theta=-\beta^*} \quad (7)$$

The following equation provides the corresponding microcrack opening displacement (δ^{micro}):

$$\delta^{micro} = V^{+} - V^{-} \tag{8}$$

$$\delta^{micro} = 8\sqrt{\frac{r}{2\pi}}\frac{K}{E} \tag{9}$$

As the microcrack initiates in the interfacial region, the stress intensity factor K, elasticity modulus E and r is replaced with $K^{Interface}$, E^{Int} and $l/2$ (as the total length of microcrack is assumed to be l as in Figure 3). When the microcrack reaches a critical length (i.e, $l = l_c$), the corresponding fracture toughness and crack opening displacement reaches their critical value (K_{Ic}^{Int}, δ_c) and is given by,

$$\delta_c^{micro} = 4\sqrt{\frac{l_c}{\pi}}\frac{K_{Ic}^{int}}{E^{Int}} \tag{10}$$

Microcracks are nucleated in concrete structure when the applied load reaches 80% of peak load. When the applied load reaches the peak load, the microcrack becomes critical and it coalesces with the macrocrack. Figure 3 represents the existence of the microcrack at the macrocrack tip considered in this study.

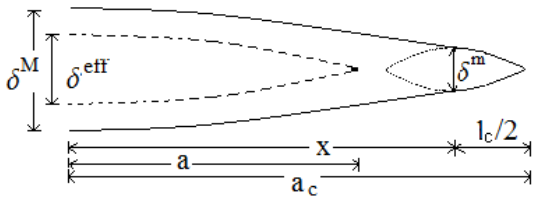

Figure 3: Representation of microcrack and macrocrack at peak load.

The macrocrack length and the stress corresponding to the peak load (P_{peak}) is represented as the critical macrocrack length (a_c) and peak stress (σ_p). The crack length corresponding to the peak load is determined by knowing the crack mouth opening displacement (δ_p) at the peak load. The following equation provides the crack opening displacement at any point (x) along the macrocrack:

$$\delta^{macro} = \frac{4\sigma_p a_c}{E} g_2\Big(\frac{a_c}{D}\Big) g_3\Big(\frac{x}{a_c}, \frac{a_c}{D}\Big) \tag{11}$$

where σ_p is the stress corresponding to the peak load, E is the elastic modulus of concrete, D is the depth of the specimen and the geometric factors $g_2(\frac{a_c}{D})$ and $g_3(\frac{x}{a_c}, \frac{a_c}{D})$ for beam specimen are taken from standard reference [5]

From Figure 3, it is clear that the crack opening displacement due to the macrocrack at ($x = a_c - l_c/2$) will be equal to the crack opening displacement due to the microcrack at $r = l_c/2$.

The critical microcrack length is determined by equating both the crack opening displacements that are given by Equations 10 and 11. The solution of the following equation gives the critical microcrack length.

$$\delta^{macro}|_{x=(a_c-\frac{l_c}{2})} = \delta^{micro}|_{r=\frac{l_c}{2}} \tag{12}$$

$$\frac{4\sigma_p a_c}{E} g_2\Big(\frac{a_c}{D}\Big) g_3\Big(\frac{x}{a_c}, \frac{a_c}{D}\Big) = 4\sqrt{\frac{l_c}{\pi}}\frac{K_{Ic}^{Int}}{E^{Int}} \tag{13}$$

As seen from the above equation, the critical microcrack length can be obtained by knowing the fracture toughness and elastic modulus of the interfacial zone. In the next section, procedure for estimating the interfacial properties is explained.

3 Interfacial fracture toughness

The lower density of cement particles around the aggregates makes the interface weaker. The initiation and propagation of a microcrack depends on the toughness of the interface. Hillemier and Hilsdor [6] conducted experiments and analytical investigations to determine the fracture properties of hardened cement paste, aggregate, and cement-paste interface. Huang and Li [7] considered the nucleation of a crack along the interface of aggregate and mortar and derived a relation between the effective toughness of the material and the mortar in terms of volume fractions by considering the crack deflection and interfacial cracking effects, which is

$$\frac{K_{IC}}{K_{IC}^{m}} = \sqrt{1 + 0.87(V_f(ca))} \sqrt{\frac{1}{1 - (\pi^2/16)V_f(ca)(1 - \nu_{eff}^2)}} \tag{14}$$

where K_{IC} is the fracture toughness of concrete, K_{IC}^{m} is the fracture toughness of mortar, $V_f(ca)$ is the volume fraction of coarse aggregate, and ν_{eff} is the Poisson's ratio of concrete. In this work, a relation between the toughness of matrix and cement paste is derived by suitably modifying and replacing the fracture toughness of concrete and mortar with those of mortar and cement paste. Also, the volume fraction of coarse aggregate and Poisson's ratio of concrete is replaced with that of fine aggregate and Poisson's ratio of mortar which takes the form

$$\frac{K_{IC}^{m}}{K_{IC}^{cp}} = \sqrt{1 + 0.87(V_f(fa))} \sqrt{\frac{1}{1 - (\pi^2/16)V_f(fa)(1-\nu_m^2)}} \quad (15)$$

The fracture toughness of cement paste - aggregate interface is much lower than that of cement paste. Hillemeier and Hilsdorf [6] conducted experiments to determine the fracture toughness of the interface and the cement paste and observed the toughness of the interface to be 0.4 times of the cement paste (ie, $K_{IC}^{Int} = 0.4K_{IC}^{cp}$) which is used in the present study.

4 Interfacial elastic modulus

The elastic modulus of the interface is another major parameter used to define the critical microcrack length (l_c) and is reported to be 0.7 times the elastic modulus of cement paste (E_{cp}) [8] and is used in this study. Hashin [9] obtained a relation between the elastic modulus of homogeneous material with and without inclusion, based on volume fraction and modulus of the inclusion by considering the change in the strain energy of a loaded homogeneous body due to the insertion of inhomogeneities using the variational theorems in the theory of elasticity. Accordingly, the relation between the elastic modulus of concrete and mortar is expressed as,

$$\frac{E}{E_m} = \frac{V_f(m)E_m + (1 + V_f(ca))E_{ca}}{(1 + V_f(ca))E_m + V_f(m)E_{ca}} \quad (16)$$

where $V_f(m)$ and $V_f(ca)$ are the volume fraction of mortar and coarse aggregate and E, E_m, and E_{ca} are the elastic modulus of concrete, mortar, and coarse aggregate respectively. The above equation can be simplified to the form,

$$V_f(m)E_m^2 + [1 + V_f(ca)]E_m[E_{ca} - E] - V_f(m)E_{ca}E = 0 \quad (17)$$

The elastic modulus of the mortar is obtained by solving the above quadratic equation. The relationship between the modulus of elasticity of mortar and cement paste is obtained in a similar manner by replacing the material properties of concrete and mortar with the properties of mortar and cement paste. Also, the volume fraction of coarse aggregate and mortar is replaced with those of fine aggregate and cement paste. The modulus of elasticity of cement paste is determined by solving the following quadratic equation.

$$V_f(cp)E_{cp}^2 + [1 + V_f(fa)]E_{cp}[E_{fa} - E_m] - V_f(cp)E_{fa}E_m = 0 \quad (18)$$

where $V_f(cp)$ and $V_f(fa)$ are the volume fraction of cement paste and fine aggregate and E_m, E_{cp}, and E_{fa} are the elastic modulus of mortar, cement paste, and fine aggregate respectively.

5 Post-peak macro behavior of concrete

The effects of microcracks on the macro behavior of plane concrete is studied through its post-peak response in this section. A relationship is obtained between the applied stress (σ) and the crack opening displacement (δ^M) along the failure plane, which occurs due to the propagation of the dominant crack.

The micro and macrocrack profiles at the peak load are represented in Figure 3. At peak load, the microcrack becomes critical and reaches a length l_c and coalesces with the macrocrack a. The macrocrack corresponding to the peak load is represented as a_c. When the crack reaches a the corresponding crack mouth opening displacement (CMOD) is given by [5], as shown in Figure 3.

$$\delta^{eff} = \frac{4\sigma a}{E} g_2\Big(\frac{a}{D}\Big) \quad (19)$$

where δ^{eff} is the crack opening displacement when the macrocrack reaches the length a as shown in Figure 3. The crack opening displacement corresponding to the peak load (ie, when the crack reaches a_c) (δ^M) can be approximated to the sum of δ^{eff} and the crack opening due to the microcrack (δ^m) as depicted in Figure 3.

$$\delta^M = \delta^{eff} + \delta^m \text{ or } \delta^{eff} = \delta^M - \delta^m \quad (20)$$

Replacing δ^{eff} in Equation 19 by Equation 20 yields to the following equation

$$\delta^M - \delta^m = \frac{4\sigma a}{E} g_2(\frac{a}{D}) \quad (21)$$

Thus, the crack opening displacement due to the macrocrack takes the following form

$$\delta^M = \frac{4\sigma a}{E} g_2(\frac{a}{D}) + \delta^m \quad (22)$$

By substituting $a = (a_c - l_c)$ and also by replacing $a_c = K_{Ic}^2/\sigma\pi g_1\left(\frac{a_c}{D}\right)^2$, the macrocrack opening displacement simplifies to the following form

$$\delta^M = \frac{4}{\pi}\frac{K_{Ic}^2}{E\sigma_p(\sigma/\sigma_p)}\left\{\frac{g_2\left(\frac{a_c-l_c}{D}\right)}{\left(g_1(a_c/D)\right)^2}\right\} \left[1 - \left(\frac{\sigma}{\sigma_p}\right)^2 \frac{\sigma_p^2 l_c \pi}{K_{Ic}^2}\left\{g_1\left(\frac{a_c}{D}\right)\right\}^2\right] + \delta^m \quad (23)$$

where K_{Ic} is the fracture toughness of the material and δ^m is the microcrack opening displacement when the microcrack becomes critical (l_c) and is given by Equation 10. Equation 23 is used to predict the post-peak behavior of concrete.

6 Analysis of experimental data

The interfacial properties, such as the modulus of elasticity and fracture toughness and the critical microcrack length as discussed in the previous section, are evaluated for normal strength concrete used by researchers in their experimental program. The following experimental data is considered in this analysis: Bazant and Xu [10] and Shah and Chandra Kishen [11]. In both research works mentioned above, tests have been carried out on beams of three different sizes (designated as small, medium, and large) which are geometrically similar under three point bending. Table 1 shows the dimensions of the beams, the peak stress, and the crack mouth opening displacement (CMOD) at peak load. The material properties, including the fracture toughness and elastic modulus as reported in these experimental works, are given in Table 2.

Table 1: Geometry and material properties of specimens

Specimen Designation	Depth	Span	Peak stress	CMOD at peak load
	D	S	σ_p	δ_p
	mm	mm	N/mm^2	mm
S [11]	76	190	4.476	0.0567
M [11]	152	380	3.589	0.0743
L [11]	304	760	3.338	0.0483
S [10]	38.1	95	4.750	0.0270
M [10]	76.2	191	3.833	0.0354
L [10]	152.4	381	3.364	0.0436

S-Small, M-Medium, L-Large

Table 2: Material properties of concrete and Interface

Fracture toughness		Elastic modulus		Ref.
$MPa\sqrt{mm}$		N/mm^2		
Concrete	Interface	Concrete	Interface	
K_{Ic}	K_{Ic}^{Int}	E	E^{Int}	
44.6	16.76	30000	5413.5	[11]
32.0	12.45	27120	5488.7	[10]

As discussed in the previous sections, the interfacial properties of concrete depends on the volume fraction of each of its constituents. The interfacial fracture toughness, the interfacial elastic modulus, and the critical microcrack length, calculated using the above mentioned

procedure, are tabulated in Table 2 and 3. It is seen that the interface is the weaker region and is therefore more prone to cracking and that justifies the analysis of the interfacial region. Furthermore, as reported in the literature [5], if the interface is weaker than the coarse aggregates, the crack propagates around the aggregate. In Table 2, it is also observed that for a particular concrete mix, the computed interfacial properties remain constant.

As reported in Table 3, the critical microcrack length is found to be dependent on the properties of the interface as well as the geometry of the specimen. Also, it is found to be increasing with the size of the specimen, even though the interfacial properties remain the same. Also, Mobasher et al. [12] have reported that 80% of microcracks is smaller than 1.5 mm in length. The critical length of microcrack is found to be comparable with the size of the fine aggregate and cement particles. Further, the critical microcrack length is normalized with the depth of beam as shown in Table 3. It is seen that this normalized value remains almost constant for a given mix of concrete and could be treated as a material property.

Table 3: Critical microcrack length

Specimen Designation	Microcrack Length l_c (mm)	l_c/D 10^{-2} $-$
S [11]	0.3659	0.40
M [11]	0.5780	0.38
L [11]	1.0910	0.36
S [10]	0.2370	0.62
M [10]	0.4540	0.60
L [10]	0.9167	0.60

S-Small, M-Medium, L-Large

7 Validation of the proposed model

The model, proposed to determine the post-peak macro behavior of the concrete specimen using the microscopic properties as represented by Equation 23, is validated for different concretes mentioned earlier in this section. As shown in Table 3, this model makes use of the interfacial properties as determined in the previous sections. Figure 4 and 5 show the post-peak behavior, determined by considering the effect of microcracks for different concretes, as predicted by the proposed model. The experimentally obtained results are also superposed on the same plots. These plots are normalized with the peak stress reported in Table 1 for the ordinates and critical crack opening displacement (δ_c) obtained from experiments for the abscissa. It is seen that there is a good match with the experimental results, thereby validating the proposed model.

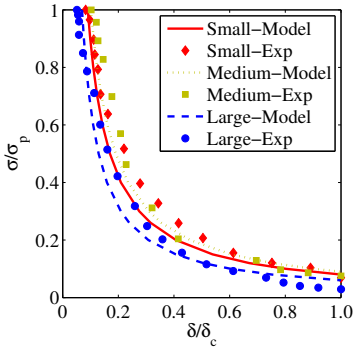

Figure 4: Comparison of post-peak behavior for concrete between proposed model and experiment [11]

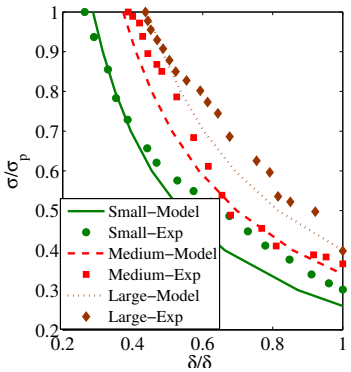

Figure 5: Comparison of post-peak behavior for concrete between proposed model and experiment [10]

8 Sensitivity analysis

Sensitivity analysis is a way to predict the outcome of decision, if a situation turns out to be different compared to the key prediction.

This method quantifies the amount of contribution of each input parameter to the output. In this study, the fracture toughness of the interface, elastic modulus of the interface, elastic modulus of concrete, the macrocrack length, and the peak stress are considered as random variables. The probability distribution as well as the statistical properties of the random variables considered in this study are listed in Table 4.

Table 4: Statistical parameters used and the results obtained in sensitivity analysis

Parameters	Mean	Standard deviation	Coefficient of sensitivity
	μ	σ	C_s
E	27120	2712	20.5
K_{IC}^{Int}	12.45	1.245	20.3
a	15.58	1.558	17.8
E^{Int}	5488.7	548.87	17.8
σ_p	4.75	0.475	17.7

Since all the random variables are positive definite, their distribution are taken to be log-normal. Also, the standard deviation of all random variables are taken as ten percent of their corresponding mean values. The mean value of each variable is taken from the experimental data reported by Bazant and Xu [10]. Also, the geometric factors $g_2(\frac{a_c}{b})$ and $g_3(\frac{x}{a_c}, \frac{a_c}{b})$ are taken as 1.8 and 0.1 as they are found to be approximately the same for all specimens.

Using statistical data, ensembles of 50,000 values of each random variable are generated. The values of critical microcrack length (l_c) are simulated five times (as five variables are considered), keeping one of the five independent variables as random at a time and others at their mean value. For all the five cases, a cumulative probability distribution (CDF) is plotted for the critical microcrack length (l_c), as in Figure 6. The parameter, corresponding to the curve with the least slope, would be the most sensitive one. As seen from this figure, the elastic modulus of concrete and the fracture toughness of the interface are the most sensitive parameters in the determination of the critical microcrack length.

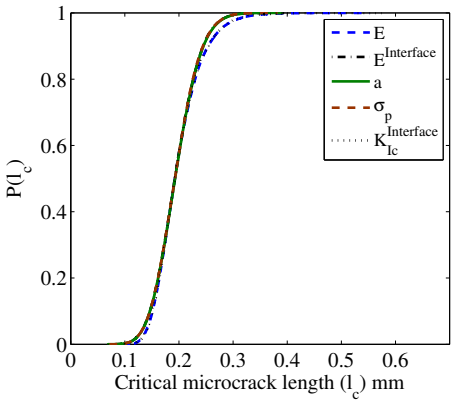

Figure 6: Probability distribution curves of the critical microcrack length (l_c) for different random variables

The coefficient of sensitivity (C_s) is computed to quantify the sensitivity of each parameter and is evaluated using

$$C_{s_i} = 100\frac{C_{v_i}^2}{C_v} \tag{24}$$

where C_{v_i} is the coefficient of variation of the dependent variable when i^{th} independent variable is considered as random with all others at their mean value and C_v is the coefficient of variation when all independent variables are taken as random.

The results of the coefficient of sensitivity are shown in Table 4. From this table it is clearly seen that the elastic modulus of concrete and the fracture toughness of the interface are the most sensitive parameters in the determination of the critical microcrack length. Similar results are also observed from the cumulative distribution of the critical microcrack length, as shown in Figure 6.

9 Summary

In this study, a critical microcrack length parameter is defined and an expression is derived by analyzing the crack opening displacement at micro and macro scales. The critical microcrack length is further used in developing a fracture model for plain concrete to study the post-peak behavior. The proposed fracture model is

validated using available experimental data. It is seen that the proposed fracture model predicts the post-peak response of plain concrete very well. For a particular mix of concrete, the ratio of critical microcrack length to the specimen depth is found to be constant and can be used as a material property. Through a deterministic sensitivity analysis, it is found that the fracture toughness of the interface and elastic modulus of concrete are the most sensitive parameters influencing the post-peak behavior of concrete.

REFERENCES

[1] JC Maso. *Interfacial transition zone in concrete, RILEM report*, volume 11. CRC Press,UK, 2004.

[2] Iulia Carmen Mihai and Anthony Duncan Jefferson. A material model for cementitious composite materials with an exterior point eshelby microcrack initiation criterion. *International Journal of Solids and Structures*, 48(24):3312–3325, 2011.

[3] Farhad Ansari. Mechanism of microcrack formation in concrete. *ACI Materials Journal*, 86(5):459–464, 1989.

[4] JGM Van Mier and A Vervuurt. Numerical analysis of interface fracture in concrete using a lattice-type fracture model. *International Journal of Damage Mechanics*, 6(4):408–432, 1997.

[5] Surendra P Shah, Stuart E Swartz, and Chengsheng Ouyang. *Fracture mechanics of concrete: applications of fracture mechanics to concrete, rock and other quasi-brittle materials*. John Wiley & Sons, NY, 1995.

[6] B Hillemeier and HK Hilsdorf. Fracture mechanics studies on concrete compounds. *Cement and Concrete Research*, 7(5):523–535, 1977.

[7] J Huang and VC Li. A meso-mechanical model of the tensile behavior of concrete. part II: modelling of post-peak tension softening behavior. *Composites*, 20(4):370–378, 1989.

[8] CC Yang. Effect of the transition zone on the elastic moduli of mortar. *Cement and Concrete Research*, 28(5):727–736, 1998.

[9] Zvi Hashin. The elastic moduli of heterogeneous materials. *Journal of Applied Mechanics*, 29(1):143–150, 1962.

[10] Zdenek P Bazant and Kangming Xu. Size effect in fatigue fracture of concrete. *ACI Materials Journal*, 88(4):390–399, 1991.

[11] S G Shah and J. M. Chandra Kishen. Fracture properties of concrete–concrete interfaces using digital image correlation. *Experimental Mechanics*, 51(3):303–313, 2011.

[12] B Mobasher, H Stang, and SP Shah. Microcracking in fiber reinforced concrete. *Cement and Concrete Research*, 20(5):665–676, 1990.